J Nanostruct 15(4): 1577-1587, Autumn 2025

RESEARCH PAPER

# Thermal Decomposition Behavior and Kinetic Evaluation Chitosan/PEO Blend Films Reinforced with Silver Nanoparticles

***Mujalli A. H. J., Najwa J. Jubier****

*Department of Physics, College of Science, Wasit University, Wasit, Iraq*

**ARTICLE INFO**

***Article History:***
*Received 19 June 2025*
*Accepted 07 August 2025*
*Published 01 October 2025*

***Keywords:***
*Chitosan*
*Coats–Redfern method*
*Kinetics*
*Polyethylene oxide*
*Silver nanoparticles*

**ABSTRACT**

This study aims to evaluate the thermal decomposition behavior and kinetic parameters of chitosan/polyethylene oxide (CS/PEO) blend films reinforced with different concentrations (1%, 3%, and 5%) of silver nanoparticles (AgNPs). Samples were fabricated using the solution casting method and characterized via thermogravimetric analysis (TGA), derivative thermogravimetry (DTG), differential scanning calorimetry (DSC), and kinetic modeling using the Coats–Redfern method; the degradation took place using a heat rate of 10° C/min in a nitrogen atmosphere. DSC results supported the thermal stability evaluation by revealing a progressive increase in the glass transition temperature (Tg), from 156.7 °C for pure chitosan (S1) to 192.3 °C for the CS/PEO blend (S3), with a peak of 214.5 °C for the 3% AgNP-reinforced sample (S5), indicating enhanced polymer chain restriction and improved thermal resistance. The activation energies (Ea) varied significantly across the samples: 73.59 kJ/mol for pure chitosan (S1), 81.07 kJ/mol for pure PEO (S2), and 79.89 kJ/mol for the 50:50 CS/PEO blend (S3). Upon AgNP incorporation, the highest value of Ea was found at 3% concentration to be (78.76 kJ/mol). The results demonstrate a non-linear behavior, indicating that AgNPs contribute to thermal stability at moderate concentrations but catalyze degradation at higher amounts. Thermodynamic parameters revealed positive enthalpy (ΔH) and negative entropy (ΔS) values, indicating an endothermic degradation process with a more ordered transition state. A strong linear correlation between Ea and ln A confirmed the presence of a kinetic compensation effect, reflecting the complex interplay between structural reinforcement and catalytic facilitation.

**How to cite this article**
*Mujalli A. H. J., Najwa J. Jubier* . Thermal Decomposition Behavior and Kinetic Evaluation Chitosan/PEO Blend Films Reinforced with Silver Nanoparticles. J Nanostruct, 2025; 15(4):1577-1587. DOI: 10.22052/JNS.2025.04.008*

## INTRODUCTION

Environmental pollution or disruption nowadays has become a serious problem in the world. Needless to say, the polymer industry currently faces numerous problems related to the recycling or disposal of polymer waste. Therefore, the importance of developing materials without any disturbance to the earth's environment is growing, even in the polymer industry. Among these problems, natural polymers have undergone a reevaluation regarding their ability to biodegrade. Chitosan is classified as a natural polymer due

* *Corresponding Author Email: njassim@uowasit.edu.iq*

to the presence of a degradable enzyme; it is extracted from chitin by removing its acetamide groups in a concentrated alkali solution. Due to its strong hydrogen bonds, chitosan is insoluble in water. Despite chitosan's many advantages as a biomaterial, its insolubility in water and incompatibility with most biodegradable polymers limit its use. This has been partially overcome by extensive efforts to improve its water solubility and compatibility with other polymers [1, 2].

Chitosan (CS) has been widely used in biomedical applications, like cancer therapy. Bone/skin regeneration and wound dressings [3–5]. Also, chitosan is expected to be beneficial in the development of composite materials, such as blends or alloys with other polymer materials, because chitosan has many functional properties [2]. On the other hand, poly (ethylene oxide) (PEO) is s bio-inert polymer of Ethylene oxide that is commercially available in a wide range of molecular weights (20,000–8,000,000), a semi-crystalline, water-soluble, non-ionic, biocompatible polymer of great industrial importance. It is used in organic–inorganic hybrid materials in the field of functional coatings with superior barrier properties [6, 7].

Despite favorable properties of PEO, when blended with a variety of polymers, such as rigid, biocompatible polymers, the resulting materials can have significantly improved flexibility and mechanical strength [1]. Blending chitosan with PEO has been extensively investigated in recent years, with several studies confirming improvements in thermal stability and mechanical properties due to synergistic molecular interactions between the polymers [8]. Such alterations can be reviewed excellently with the help of thermal analysis methods, to be particular thermogravimetric analysis ( TGA ) that helps get specific information regarding the dissemination character as well as therapeutic stability of the polymerized material.

So far, it has been evidenced that the introduction of silver nanoparticles (AgNPs) into CS/PEO matrices contributes to a tremendous improvement in the thermal conductivity of the ensuing composite materials. AgNPs have high surface-to-volume ratio, and good thermal conductivity that helps in enhancing their ability to transfer heat within their material, slowing down the aspect of thermal degradation. The reported results show that 5% AgNPs had led to an increment in thermal conductivity that rose to 0.099 W/m K as compared to 0.023 W/m K before the introduction of AgNPs. [9]. The phenomenon of the positive effect of nanoparticles reinforcement in polymer materials is regarded as a well-established phenomenon of science and fact not confined to a particular material form. The same behavior has been established in other systems, such as boron nitride in epoxy matrices (Thamir et al., 2019) or silica nanoparticles in thermosetting resins (Al-Bayaty et al., 2020), hence reflecting the universality of methods of nanoparticle reinforcement [10,11].

On the other hand, in recent research, it was also revealed that nanoparticles act as catalysts promoting the degradation of polymer material and lowering the value of an activation energy during the thermal decomposition of polymers (Sharma et al., 2014). The importance of knowing the working mechanisms of these nanoparticle behavior is vital to the overall optimization of performance of together composite materials since this diversity in functionality gives rise to a huge range of responses. [12].

In this regard, this research objective will be able to assess the thermal conductivity of chitosan/PEO nanocomposite films and determine how concentrations of silver nanoparticles affect thermodynamic properties through TGA and DSC analysis. In determining the energy and the mechanism of decomposition per formulation, the Coats Redfern analysis technique will be used to examine the thermal degradation kinetics.

To determine the kinetic and thermodynamic parameters of the degradation process, Thermal analysis techniques such as thermogravimetric analysis (TGA) and derivative thermogravimetric analysis (DTG) are widely used to investigate the thermal behavior and decomposition kinetics of polymeric materials. These techniques are essential for evaluating thermal stability, decomposition stages, and kinetic parameters such as activation energy (Ea), enthalpy (ΔH), entropy (ΔS), and Gibbs free energy (ΔG). Among the available kinetic models, the Coats–Redfern method is commonly used due to its accuracy and simplicity.

The thermal degradation of solids under non-isothermal conditions can be represented as:

$$A_{(solid)} + B_{\rightarrow (solid)} = C_{(volatile)} \quad (1)$$

The extent of conversion (α) is commonly calculated using the following expression:

$$\alpha = (m_0 - m_t) / (m_0 - m_\infty) \quad (2)$$

Where, $m_o$ = initial mass of the sample , $m_t$ = mass at time t, and $m_\infty$ = final mass after decomposition

During TGA analysis with a constant heating rate (β), the rate of conversion is given by:

$$dx/dt = \beta \times dx/dT = K(T) \times f(x) \quad (3)$$

Where: x= degree of conversion, f(x)= reaction model, and K(T)= temperature-dependent rate constant

The rate constant K(T) follows the Arrhenius equation:

$$K(T) = A \times \exp(-E_a / RT) \quad (4)$$

Where: $E_a$ = activation energy (kJ/mol), A = pre-exponential factor, R = universal gas constant

For kinetic analysis, the Coats–Redfern equation is applied as:

$$\ln[-\ln(1-\alpha)/T^2] = \ln[(AR/\beta E_a) \times (1 - 2RT/E_a)] - E_a/R$$

Activation energy can be calculated using the slope of linear relationship by recording the left-side of the equation (ln [ln (1 1- a)/T 2]) on the y axis and the magnitude (1000/T) on the X axis. Intercept at y-axis can also be used to obtain frequency factor (A) by plugging the values of activation energies to the following equation

$$\text{Intercept} = \ln[(AR/\beta E_a) \times (1 - 2RT/E_a)]$$

The model has been efficiently applied in current examinations to determine the kinetics parameters of polymer nanocomposites [10, 13]. Other causes of the thermal behavior of polymer nanocomposites can be obtained besides kinetics which is thermodynamic parameters such as enthalpy of activation (ΔH), entropy of activation (Delta S) and Gibbs free energy of decomposition (ΔG). These were calculated using the following relationships:

$$\Delta H = Ea - R \times Tpeak$$

$$\Delta S = R \times [\ln(h \times A_0 / K_b \times T_{peak}) - 1$$

$$\Delta G = \Delta H - T_{peak} \times \Delta S$$

Where: R = Universal gas constant, $T_{peak}$ = Peak temperature from DTG curve, h = Planck constant, $K_b$ = Boltzmann constant [14].

These thermodynamic parameters are fundamental for understanding the thermal decomposition mechanisms of polymer-based nanocomposites and can support further interpretation of thermal behavior under non-isothermal conditions.

## MATERIALS AND METHODS

### *Materials*

The components in this work are chitosan (CS), polyethylene oxide (PEO) and silver nanoparticles (AgNPs). Chitosan, was obtained from Nano Chemazone Inc. Polyethylene oxide (PEO), identified by CAS No. 68441-17 8, has a molecular formula of $C_{51}H_{102}O_{21}Si_2$, appears as a white powder, and has a melting point ranging from 66-70°C. Its true density is between 1.15-1.22 kg/L, and it decomposes thermally at 423-425°C. This polymer was sourced from Gree Industry. The silver nanoparticles (AgNPs) used in this study have an average particle size of 50-60 nm, with an assay of 99.9% purity, a spherical morphology, and a bulk density of 0.35 g/cm³. These nanoparticles were supplied by Sky Spring Nanomaterials Inc. Acetic acid (1% solution) was used as a solvent for chitosan, while distilled water was employed as a solvent for polyethylene oxide.

### *Preparation of Pure and Composite Films*

Films of pure chitosan (CS), pure polyethylene oxide (PEO), and their blend were prepared using

the solvent casting method. Chitosan (2 wt. %) was dissolved in 1% acetic acid solution under magnetic stirring for 6 hours at room temperature. PEO (2 wt%) was separately dissolved in distilled water under stirring for 6 hours. The two polymer solutions were mixed in a 1:1 ratio (CS: PEO) and stirred for 30 minutes to ensure homogeneity. For the composite films, silver nanoparticles (AgNPs) were incorporated at concentrations of 1%, 3%, and 5% (w/w based on total polymer weight). The AgNPs were ultrasonically dispersed in the polymer blend solution for 1 hour to ensure uniform distribution. The final mixtures were poured into 14 cm diameter Petri dishes and dried at room temperature for 5 days. The dried films were then carefully peeled off and stored in a desiccator until further analysis.

## RESULTS AND DISCUSSION

*TGA/DTG Analysis of Chitosan/PEO: Pure, Blend, and AgNP-Reinforced Films*

Figs. 1 and 2 present the thermogravimetric analysis (TGA) and derivative thermogravimetric (DTG) curves for the pure chitosan, pure polyethylene oxide, and their blend samples (S1 to S3), were incorporated with nano Ag concentrations of 1%, 3%, and 5% (S4-S6) which illustrate their thermal degradation behavior under a nitrogen atmosphere. In the TGA curves (Fig. 1), all samples exhibit a characteristic three-step degradation pattern. The first stage occurs between 30°C and 100°C, associated with the evaporation of physically adsorbed moisture, particularly evident in hydrophilic systems like chitosan and PEO. The second major weight loss occurs between 200°C and 320°C, corresponding to the initial thermal decomposition of the polymer backbones. For chitosan, this includes dehydration, deamination, and depolymerization, whereas PEO undergoes chain scission and melting-induced degradation. The third stage, extending beyond 400°C, is attributed to the formation of char residues, especially from chitosan-rich structures.

These observations are further substantiated by the DTG curves in Fig. 2, which provide clearer information about the rate and temperature of thermal degradation. Each sample demonstrates distinct DTG peak positions (Tpeak) corresponding to the maximum degradation rate. It was noticed that S1 exhibits multiple DTG peaks, confirming a multi-step decomposition typical of chitosan. S2, on the other hand, displays a sharp and singular DTG peak near 400°C, indicating a rapid degradation process of pure PEO.

Upon blending (S3), the DTG peak is slightly shifted, and a smoother degradation profile is observed, suggesting increased thermal stability due to polymer chain interactions. Samples S4 to

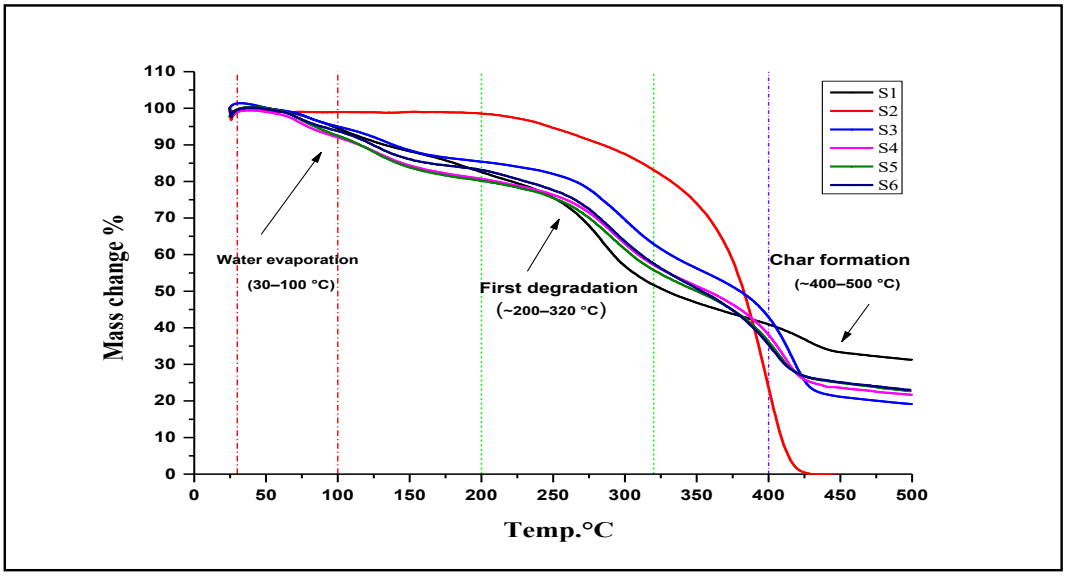


Fig. 1. Thermogravimetric analysis (TGA) curves of samples S1–S6, illustrating moisture evaporation, thermal decomposition, and char formation behavior.

S6 reinforced with AgNPs showed a progressive shift in DTG peaks toward higher temperatures, alongside reduced mass loss percentages in the TGA curves. This result indicates that the incorporation of silver nanoparticles significantly enhances the thermal stability of the composite films, likely by restricting chain mobility, increasing thermal conductivity, and promoting a more ordered decomposition mechanism.

These observations are illustrated by the numerical data in Table 1, which confirms that AgNP-reinforced samples experienced lower total mass loss and retained higher char residue compared to the unreinforced blend.

The role of silver nanoparticles as thermally resistant fillers and structural barriers within polymer matrices has been well documented in several studies. They have been shown to enhance thermal performance by restricting the mobility of polymer chains and delaying decomposition. Other reports have indicated that functionalized nanoparticles act as diffusion barriers, reducing heat transfer within the matrix and inhibiting thermal degradation [15,9].

*Differential Scanning Calorimetry (DSC) Analysis*

The DSC curves for the pure chitosan, pure polyethylene oxide, and their blend samples (S1 to S3), were incorporated with nano Ag concentrations of 1%, 3%, and 5% (S4-S6), are shown in Fig. 3. Each curve exhibits characteristic thermal transitions related to the composition

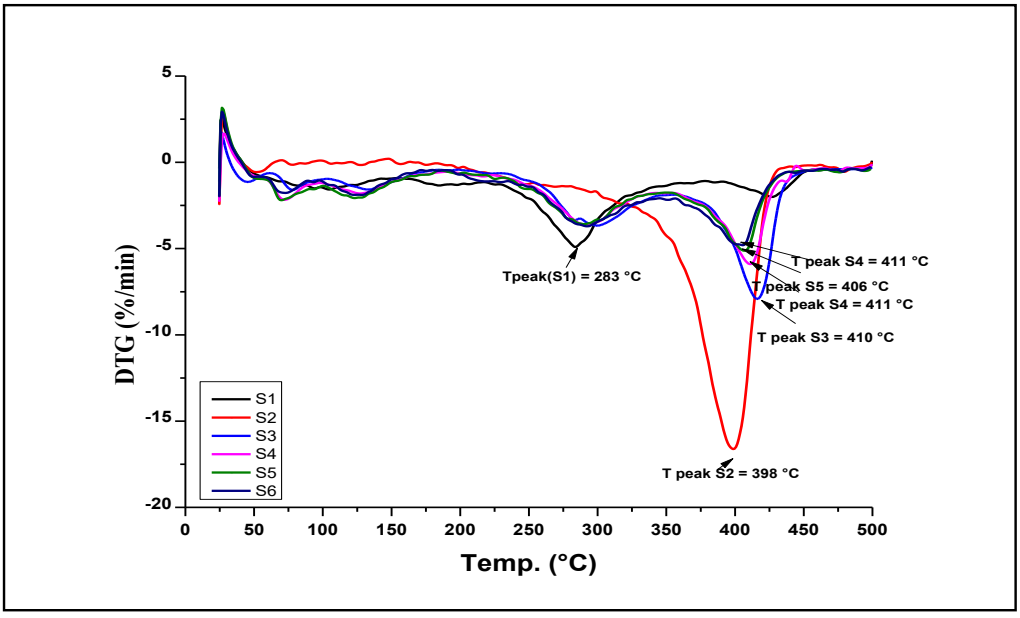


Fig. 2. DTG Curves of Samples S1–S6 Showing Thermal Decomposition Peaks under a nitrogen atmosphere.

Table1. Thermal degradation behavior from TGA/DTG analysis for prepared samples.

| Sample | AgNPs (%) | Mass Loss (%) | Main Degradation Start (°C) | DTG Peak (°C) | Residual Mass (%) |
|---|---|---|---|---|---|
| S1 | 0 | 66.42 | 230 | 283.65 | 33.58 |
| S2 | 0 | 101.87 | 330 | 398.343 | ~1.87 |
| S3 | 0 | 81.00 | 270 | 410.913 | 19.00 |
| S4 | 1% | 78.22 | 290 | 411.373 | 21.78 |
| S5 | 3% | 77.39 | 300 | 406.714 | 22.61 |
| S6 | 5% | 77.04 | 310 | 403.951 | 22.96 |

and structural features of the samples. The main observed thermal noticed include moisture evaporation, glass transition temperature (Tg), and thermal degradation.

The glass transition temperatures were identified depending on the movement of the DSC base after the initial loss of moisture, which is the region of the 1261879 alpha -relaxation. The methodology is in line with that provided by Gonzales-Campos et al, (2010) [16].

The DSC curves of the Sample S1 (100% chitosan) showed a clear endothermic peak respecting about 66.3o C, which can be attributed so far as to the evaporation of the physically adsorbed and weakly bonded hydrogen-water molecules. Clear endothermic peak can be observed at about 66.3 °C using the DSC curves of Sample S1 (100%% chitosan) and can be assigned to the evaporation of water molecules physically adsorbed and weakly hydrogen-bonded.This was followed by glass transition at approximately 156.7 °C which implied that the mobility of the polymer chain would increase.

An exothermic bump was observed around 289.7 o C, which showed rearrangement of structure and onset of thermal decomposition

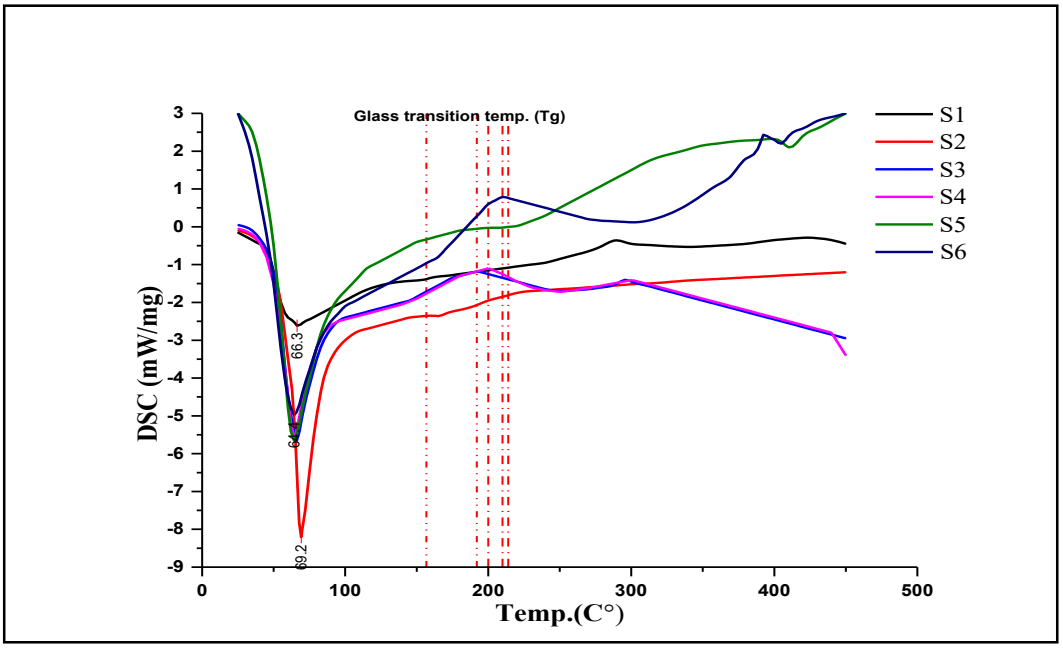


Fig. 3. DSC curves of all prepared polymer blend samples (S1–S6).

Table 2: Main Thermal Events and Transitions in DSC Thermograms.

| Sample | Sample Description | First Peak (°C) | Glass Transition (Tg) (°C) | Main Degradation Peak (°C) |
|---|---|---|---|---|
| S1 | Pure chitosan | 66.3 | 156.7 | 289.7, 424.2 |
| S2 | Pure PEO | 69.2 | - | ~380 (unclear) |
| S3 | CS/PEO blend | 66.1 | 192.3 | 295.9 |
| S4 | CS/PEO /1% AgNPs | 64.3 | 200.1 | 300.6 |
| S5 | CS/PEO/ 3% AgNPs | 64.3 | 214.5 | 399.7 |
| S6 | CS/PEO /5% AgNPs | 64.4 | 210.0 | 392.4 |

such as dehydration, deamination, and depolymerization.

A final thermal transition was detected around 424.2 °C, corresponding to the breakdown of the chitosan polymer backbone and the formation of carbonaceous char residues. These observations are in strong agreement with the thermal decomposition behavior of chitosan [17].

Based on the DSC analysis of Sample S2 (100% polyethylene oxide, PEO), a sharp endothermic peak was observed at approximately 69.2°C, corresponding to the melting of crystalline regions within the PEO matrix. In addition, a broad endothermic region was detected around 163.8°C, which is likely related to molecular rearrangement and the onset of thermal degradation processes

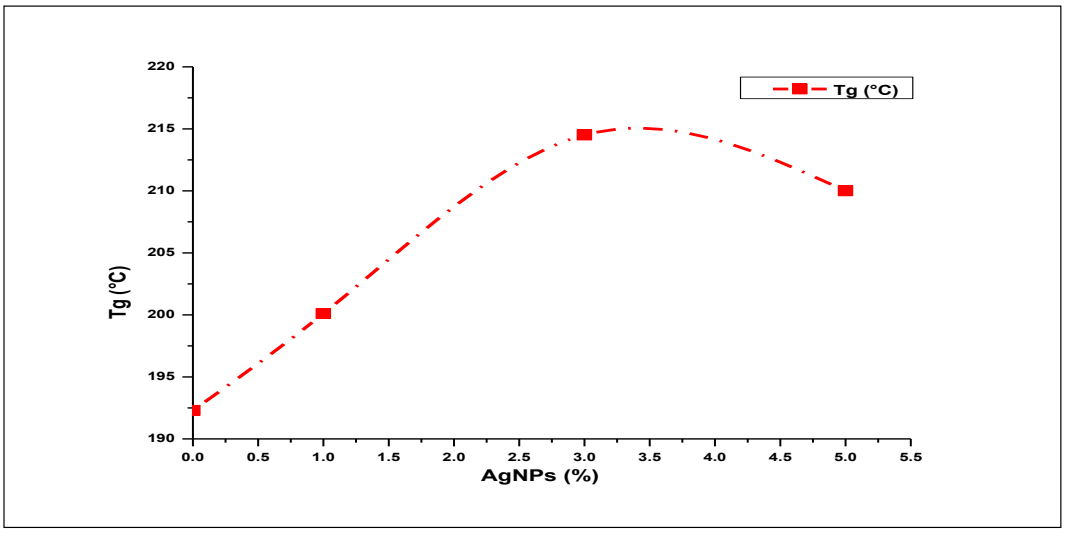


Fig. 4. Variation of Glass Transition Temperature (Tg) with AgNPs Concentration in the blend.

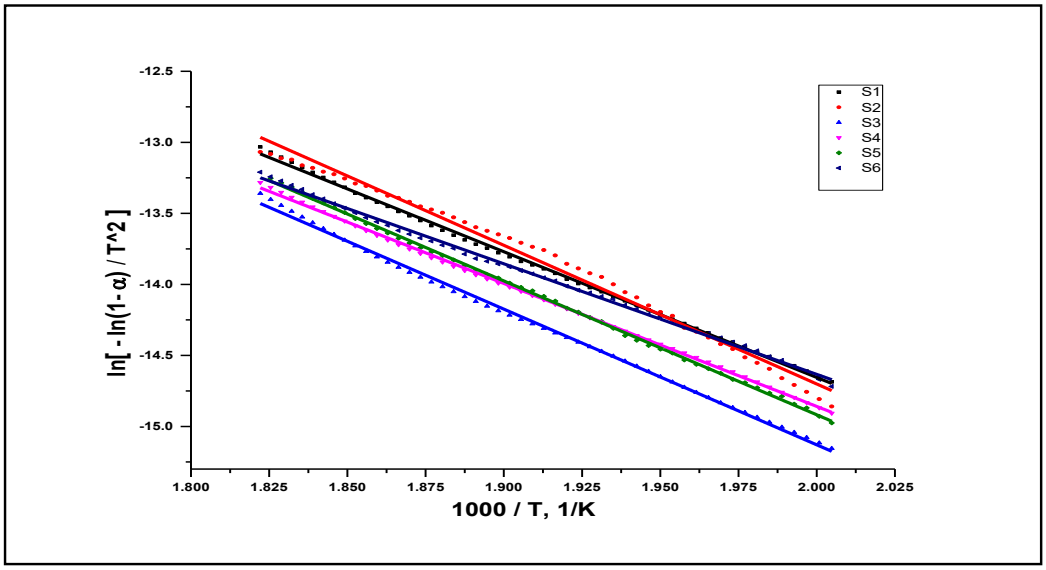


Fig. 5. Linear plots of Coats–Redfern equation for thermal decomposition of prepared samples.

[18,19].

While for blend sample S3 (50%CS / 50%PEO), it exhibited an endothermic peak at approximately 66.1°C, attributed to the evaporation of physically adsorbed water. The glass transition temperature (Tg) was shifted to around 192.3°C, indicating strong intermolecular interactions between chitosan and PEO chains. An exothermic peak was observed at 295.9 °C, suggesting partial structural reorganization before the onset of thermal degradation. These thermal behaviors are consistent with previous studies that reported improvements in thermal stability and molecular interactions in chitosan/PEO blends [20].

The three final samples (S4, S5 and S6) loaded with silver nanoparticles (Silver NPs), showed the same thermal profile with a peak pertaining to moisture evaporating at around 64.364.4C. Also, the glass transition temperature (Tg) was measured to be increased noticeably compared to the S3 sample, and it implied that AgNPs addition led to greater thermal stability and limited the mobility of polymer chains. Furthermore, a shift towards elevated values of the temperatures of onset of thermal degradation could also be observed implying better thermal stability against thermal degradation. Such findings agree with recent findings by other researchers who indicated the improvement of thermal stability in polymer blends by reinforcing Ag NPs [15,21].

Table 2 provides a summary of key thermal results for all samples, detailing main thermal transitions in DSC curves, including the first endothermic peak, glass transition, and main degradation peak. Furthermore, the relationship between the glass transition temperature (Tg) and

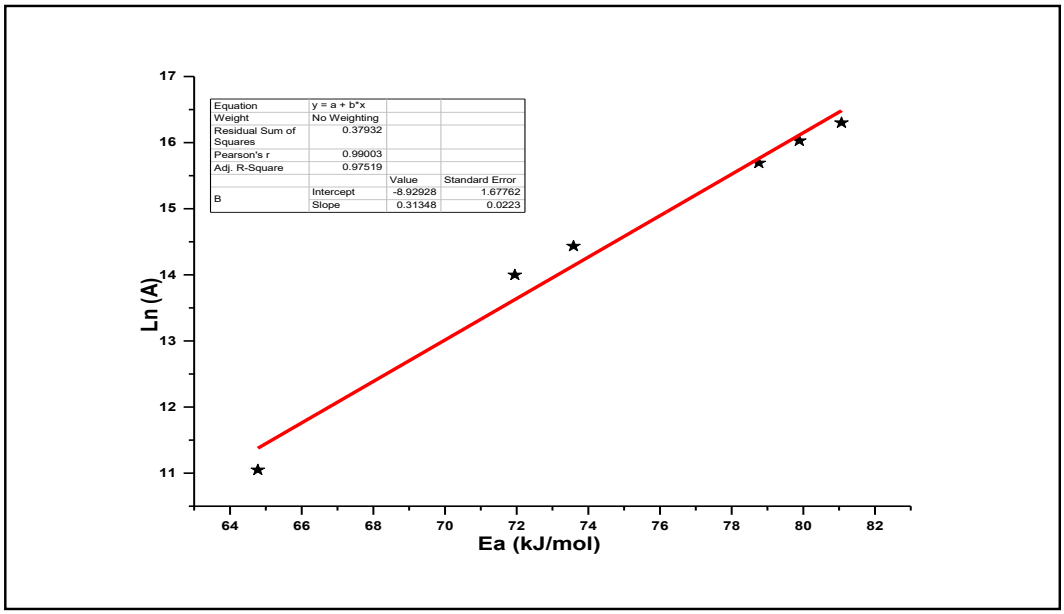


Fig. 6. Linear correlation between activation energy (Ea) and the natural logarithm of the pre-exponential factor (ln A) in prepared sample.

Table 3. Kinetic and thermodynamic parameters of prepared samples calculated using the Coats–Redfern method.

| Sample | Ea (kJ/mol) | ΔH (kJ/mol) | A ($s^{-1}$) | ΔS (kJ/mol·K) | ΔG (kJ/mol) | $R^2$ |
|---|---|---|---|---|---|---|
| S1 | 73.59 | 68.96 | 1.856e+06 | -0.13017 | 141.41 | 0.9986 |
| S2 | 81.07 | 75.49 | 1.1997e+07 | -0.11614 | 153.46 | 0.9885 |
| S3 | 79.89 | 74.23 | 9.132e+06 | -0.11978 | 155.13 | 0.9975 |
| S4 | 71.95 | 66.26 | 1.2003e+06 | -0.13383 | 157.8 | 0.9992 |
| S5 | 78.76 | 73.11 | 6.53e+06 | -0.12159 | 155.57 | 0.9994 |
| S6 | 64.78 | 59.18 | 62930 | -0.15414 | 163.51 | 0.9979 |

the silver nanoparticle (AgNPs) concentration is illustrated in Fig. 4.

*Kinetic and Thermodynamic Analysis Using the Coats–Redfern Method*

The thermal decomposition behavior of chitosan/PEO blends films, both pure and those reinforced with silver nanoparticles (AgNPs) were evaluated using the Coats–Redfern method within the temperature range of 275-320°C. The calculated kinetic and thermodynamic parameters are presented in Table 3.

All samples exhibited high linear correlation coefficients ($R^2 > 0.98$), confirming the applicability of a first-order kinetic model. The corresponding Coats–Redfern plots (Fig. 5) displayed clear linearity, enabling precise parameter extraction.

The activation energy, defined as the minimum amount of energy required to initiate the thermal degradation process, is considered a quantitative indicator of the thermal stability of polymer-based materials [22]. In the present study, the calculated activation energies (Ea) using the Coats–Redfern method showed significant variation depending on the silver nanoparticle (AgNPs) content within the chitosan/PEO matrix. As shown in Table 3, the Ea value of the unreinforced blend (S3) was 79.89 kJ/mol, serving as the baseline for comparison.

Furthermore, the sample containing 1% AgNPs (S4) exhibited a slightly lower Ea of 71.95 kJ/mol, suggesting an early catalytic influence of the silver nanoparticles on the degradation mechanism, and sample S5 (3% AgNPs) exhibits an Ea of 78.76 kJ/mol, which is comparable to that of the blend, indicating that at this concentration, AgNPs contribute more significantly to structural reinforcement than to catalysis. This enhancement in thermal resistance is attributed to improved polymer–nanoparticle interactions, which restrict chain mobility and delay the onset of decomposition.

While sample S6 (5% AgNPs) exhibited a substantial decrease in Ea to 64.78 kJ/mol and a dramatic drop in the frequency factor (A), indicating a shift toward catalytic facilitation of the degradation process. This effect can be related to either nanoparticle agglomeration or active-site saturation effects which can cause the change of thermal-degradation pathways. Other nanocomposite systems have also been reported to exhibit such behaviour where enhancing the concentration of fillers reverses the structural strengthening effect to catalytic breakdown.. This phenomenon, characterized by reinforcement at moderate nanoparticle levels and catalysis at higher concentrations, agrees with previous studies by Kumar et al. (2009) and Franco-Urquiza et al. (2020), which demonstrated that specific nanoparticle loadings can facilitate stepwise degradation or lower the activation energy of thermal decomposition through catalytic mechanisms [23,24]. A strong linear correlation ($R^2$ =~ 0.98) between activation energy (Ea) and the frequency factor (ln A) was also observed

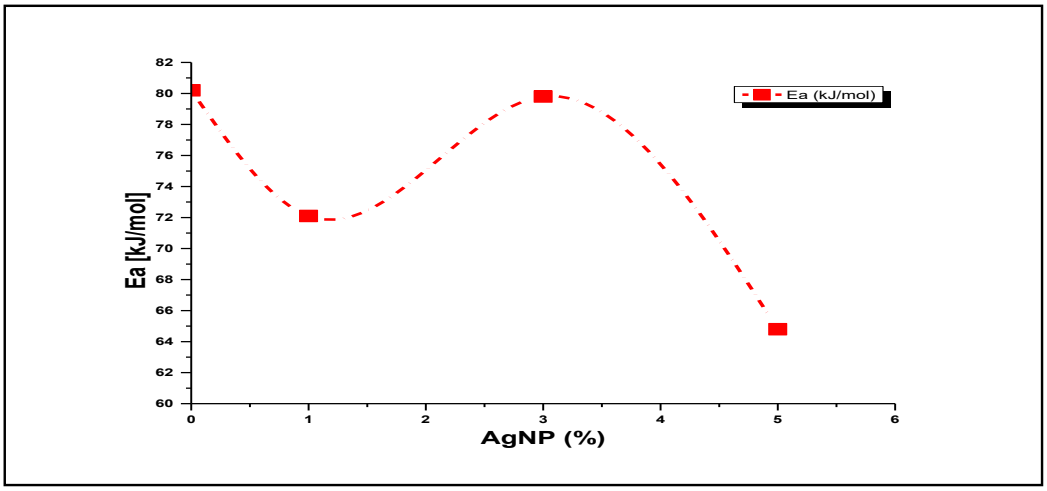


Fig. 7. Effect of AgNPs concentration on the activation energy (Ea) in prepared samples.

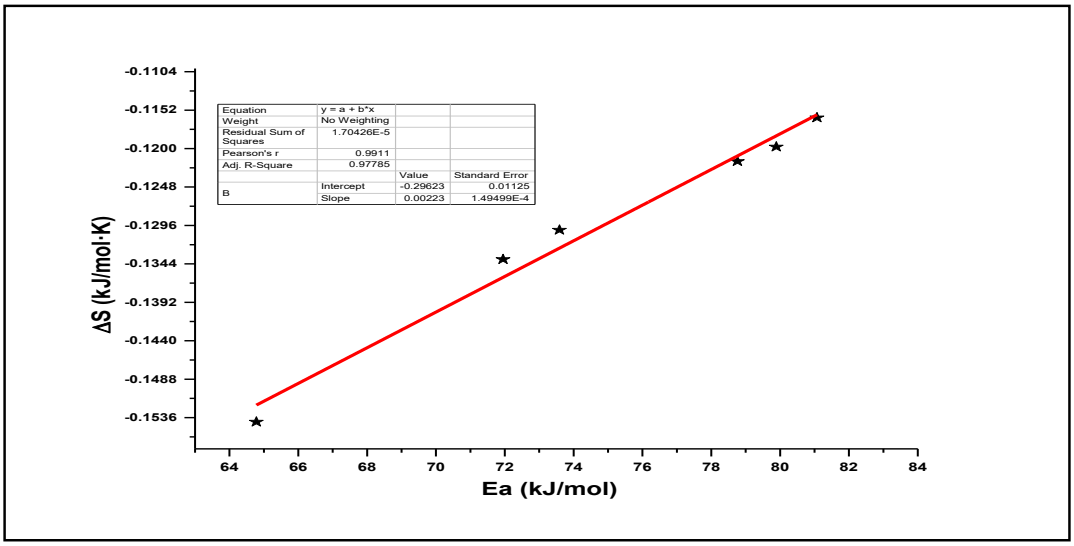


Fig. 8. Plot of activation energy (kJ/mol) versus ΔS (kJ/mol·K).

as in Fig. 6, suggesting the presence of a kinetic compensation effect [14]. This behavior has been previously documented in nanoparticle-reinforced systems, where structural reinforcement and catalytic activity interact to determine the thermal stability of the material [25]. Farhan et al. (2022) demonstrated that nanoparticle effects vary significantly with polymer matrix composition, where the same nanoparticle loading showed different behaviors depending on the specific polymer type, supporting the complex nature of nanoparticle-polymer interactions [26]. Fig. 7 illustrates the effect of AgNP concentration on the activation energy (Ea) in prepared samples.

The negative values of entropy (ΔS) indicate a more ordered transition state [27], while the positive Gibbs free energy values (ΔG) confirm the non-spontaneity of the decomposition process. Additionally, the positive enthalpy values (ΔH) reflect the endothermic nature of bond breaking within the polymer chains [28].

The relationship between activation energy (Ea) and entropy (ΔS) is illustrated in Fig. 8, showing a strong linear correlation ($R^2$ =0.977) that confirms the presence of an enthalpy-entropy compensation effect and validates the thermodynamic consistency of the Coats-Redfern analysis.

Thermal analysis results demonstrate the combined role of silver nanoparticles (AgNPs), which function both as structural reinforcements and catalytic agents. The delayed degradation onset and increased residual mass observed in TGA/DTG curves indicate enhanced thermal resistance, likely due to restricted polymer chain mobility and improved matrix packing induced by AgNPs. Simultaneously, the marked reduction in activation energy at higher AgNP concentrations supports the hypothesis that catalytic effects dominate, facilitating decomposition through alternative, lower-energy pathways.

## CONCLUSION

It can be concluded that further improvement in thermal resistance was shown from the DSC measurements, as the incorporation of AgNPs led to a noticeable upward shift in the glass transition temperature (Tg), particularly at 3% concentration, indicating restricted polymer chain dynamics. This thermal behavior is consistent with the findings of the TGA and kinetic analysis, which confirmed the concentration-dependent dual role of AgNPs. At intermediate concentrations (3%), AgNPs enhance thermal stability through their structural reinforcing effect, while at higher concentrations (5%), they exhibit a catalytic behavior that facilitates the thermal degradation process. The strong linear relationship between the activation energy (Ea) and the frequency factor (ln A), along with the clear correlation between the activation energies and entropy (ΔS), confirms the presence of a compensatory effect, thereby supporting

the reliability of the thermogravimetric analysis according to the Coats–Redfern model. These results contribute to a deeper understanding of the improvement of nanomaterial structures to enhance thermal performance.

## CONFLICT OF INTEREST

The authors declare that there is no conflict of interest regarding the publication of this manuscript.

## REFERENCES


1. Bostan MS, Mutlu EC, Kazak H, Sinan Keskin S, Oner ET, Eroglu MS. Comprehensive characterization of chitosan/PEO/levan ternary blend films. Carbohydr Polym. 2014;102:993-1000.
2. Sakurai K. Glass transition temperature of chitosan and miscibility of chitosan/poly(N-vinyl pyrrolidone) blends. Polymer. 2000;41(19):7051-7056.
3. Tao F, Cheng Y, Shi X, Zheng H, Du Y, Xiang W, et al. Applications of chitin and chitosan nanofibers in bone regenerative engineering. Carbohydr Polym. 2020;230:115658.
4. Mahmood HS, Jawad MK. Investigation of Chitosan/PEO Reinforced with AgNPs for Antibacterial Activity Prepared by Solution Casting Method. Annals of Tropical Medicine and Public Health. 2019;22(09):70-82.
5. Xu K, Ganapathy K, Andl T, Wang Z, Copland JA, Chakrabarti R, et al. 3D porous chitosan-alginate scaffold stiffness promotes differential responses in prostate cancer cell lines. Biomaterials. 2019;217:119311.
6. Vrandečić NS, Erceg M, Jakić M, Klarić I. Kinetic analysis of thermal degradation of poly(ethylene glycol) and poly(ethylene oxide)s of different molecular weight. Thermochim Acta. 2010;498(1-2):71-80.
7. Liu P, Chen W, Liu C, Tian M, Liu P. A novel poly (vinyl alcohol)/poly (ethylene glycol) scaffold for tissue engineering with a unique bimodal open-celled structure fabricated using supercritical fluid foaming. Sci Rep. 2019;9(1).
8. Madian NG, El-Ashmanty BA, Abdel-Rahim HK. Improvement of Chitosan Films Properties by Blending with Cellulose, Honey and Curcumin. Polymers. 2023;15(12):2587.
9. Hasan IMM, Al-Zobidy SF, A. Mahmood T, J. Kadhim N, K. Ayal A. Synthesis, Characterization and Study the Antibacterial Activity of Some Disubstutited-1,3,4-Oxadiazole Derivatives. Iraq Journal of Market Research and Consumer Protection. 2019;11(1):170-182.
10. Thamer AA, Yusr HA, Jubier NJ. TGA, DSC, DTG Properties of Epoxy Polymer Nanocomposites by Adding Hexagonal Boron Nitride Nanoparticles. Journal of Engineering and Applied Sciences. 2019;14(2):567-574.
11. Al-Bayaty SA, Al-Uqaily RAH, Jubier NJ. Using the Coats-Redfern Method during Thermogravimetric Analysis and Differential Scanning Calorimetry Analysis of the Thermal Stability of Epoxy and Epoxy/Silica Nanoparticle Nanocomposites. Journal of Southwest Jiaotong University. 2020;55(4).
12. Sharma JK, Srivastava P, Singh S, Singh G. Review on the Catalytic Effect of Nanoparticles on the Thermal Decomposition of Ammonium Perchlorate. Energy and Environment Focus. 2014;3(2):121-130.
13. Jubier NJ, Al-Jorani KR, Ali AA, Al –Bayaty SA, Al-Uqaily RAH. Thermal degradation assessment, impact strength, and hardness of combination epoxy and polystyrene powder composite. Kuwait Journal of Science. 2024;51(4):100271.
14. Study of Thermal Decomposition Behavior and Kinetics of Epoxy/Polystyrene Composites by using TGA and DSC. Journal of Xi'an University of Architecture and Technology. 2020;XII(III).
15. Murillo L, Rivero PJ, Sandúa X, Pérez G, Palacio JF, Rodríguez RJ. Antifungal Activity of Chitosan/Poly(Ethylene Oxide) Blend Electrospun Polymeric Fiber Mat Doped with Metallic Silver Nanoparticles. Polymers. 2023;15(18):3700.
16. González-Campos JB, Prokhorov E, Luna-Bárcenas G, Sanchez IC, Lara-Romero J, Mendoza-Duarte ME, et al. Chitosan/silver nanoparticles composite: Molecular relaxations investigation by dynamic mechanical analysis and impedance spectroscopy. J Polym Sci, Part B: Polym Phys. 2010;48(7):739-748.
17. Kraskouski A, Hileuskaya K, Nikalaichuk V, Ladutska A, Kabanava V, Yao W, et al. Chitosan-based Maillard self-reaction products: Formation, characterization, antioxidant and antimicrobial potential. Carbohydrate Polymer Technologies and Applications. 2022;4:100257.
18. Jakić M, Santro A, Zečić E, Perinović Jozić S. Thermal Analysis of the Biodegradable Polymer PVA/PEO Blends. Tehnički glasnik. 2024;18(2):224-228.
19. Ibrahim S, Yasin SMM, Ahmad R, Johan MR. Conductivity, thermal and morphology studies of PEO based salted polymer electrolytes. Solid State Sciences. 2012;14(8):1111-1116.
20. Neto CGT, Giacometti JA, Job AE, Ferreira FC, Fonseca JLC, Pereira MR. Thermal Analysis of Chitosan Based Networks. Carbohydr Polym. 2005;62(2):97-103.
21. Elashmawi IS, Al-Muntaser AA, Ismail AM. Structural, optical, and dielectric modulus properties of PEO/PVA blend filled with metakaolin. Opt Mater. 2022;126:112220.
22. Wellen RMR, Canedo EL. On the Kissinger equation and the estimate of activation energies for non-isothermal cold crystallization of PET. Polym Test. 2014;40:33-38.
23. Kumar AP, Depan D, Singh Tomer N, Singh RP. Nanoscale particles for polymer degradation and stabilization—Trends and future perspectives. Prog Polym Sci. 2009;34(6):479-515.
24. Franco-Urquiza EA, May-Crespo JF, Escalante Velázquez CA, Pérez Mora R, González García P. Thermal Degradation Kinetics of ZnO/polyester Nanocomposites. Polymers. 2020;12(8):1753.
25. Alshorifi FT, Alswat AA, Mannaa MA, Alotaibi MT, El-Bahy SM, Salama RS. Facile and Green Synthesis of Silver Quantum Dots Immobilized onto a Polymeric CTS–PEO Blend for the Photocatalytic Degradation of p-Nitrophenol. ACS Omega. 2021;6(45):30432-30441.
26. Farhan A, Al-Bayaty S, Hassani R, Hussein W. Kinetic of Thermal Degradation of RTV Silicon Rubber Blends Reinforced With Nanoparticles by TGA and DSC Analysis Techniques. Egyptian Journal of Chemistry. 2021;0(0):0-0.
27. Turmanova S, Genieva S, Vlaev L. Kinetics of Nonisothermal Degradation of Some Polymer Composites: Change of Entropy at the Formation of the Activated Complex from the Reagents. Journal of Thermodynamics. 2011;2011(1).
28. Sawada H. Thermodynamics of Polymerization. I. Journal of Macromolecular Science, Part C: Polymer Reviews. 1969;3(2):313-338.